Bioactive Materials 6 (2021) 810–822

Contents lists available at ScienceDirect

Bioactive Materials

journal homepage: http://www.keaipublishing.com/biomat

Calcium silicate bioactive ceramics induce osteogenesis through oncostatin M

Panyu Zhou[a,1], Demeng Xia[a,1], Zhexin Ni[b,1], Tianle Ou[c], Yang Wang[a], Hongyue Zhang[a], Lixia Mao[d], Kaili Lin[d,*], Shougui Xu[a,**], Jiaqiang Liu[d,***]

[a] Department of Emergency, Changhai Hospital, Naval Medical University, Shanghai, China
[b] Department of Gynecology of Traditional Chinese Medicine, Changhai Hospital, Naval Medical University, Shanghai, China
[c] Department of Clinical Medicine, the Naval Medical University, Shanghai, China
[d] Department of Oral & Cranio-Maxillofacial Surgery, Shanghai Ninth People's Hospital, Shanghai Jiao Tong University School of Medicine, Shanghai Key Laboratory of Stomatology, Shanghai Research Institute of Stomatology, Shanghai, China

ARTICLE INFO

Keywords:
Osteoimmune
Osteogenesis
Calcium silicate
Macrophage
Macrophage polarization

ABSTRACT

Immune reactions are a key factor in determining the destiny of bone substitute materials after implantation. Macrophages, the most vital factor in the immune response affecting implants, are critical in bone formation, as well as bone biomaterial-mediated bone repair. Therefore, it is critical to design materials with osteoimmunomodulatory properties to reduce host-to-material inflammatory responses by inducing macrophage polarization. Our previous study showed that calcium silicate (CS) bioceramics could significantly promote osteogenesis. Herein, we further investigated the effects of CS on the behavior of macrophages and how macrophages regulated osteogenesis. Under CS extract stimulation, the macrophage phenotype was converted to the M2 extreme. Stimulation by a macrophage-conditioned medium that was pretreated by CS extracts resulted in a significant enhancement of osteogenic differentiation of bone marrow mesenchymal stem cells (BMSCs), indicating the important role of macrophage polarization in biomaterial-induced osteogenesis. Mechanistically, oncostatin M (OSM) in the macrophage-conditioned medium promoted osteogenic differentiation of BMSCs through the ERK1/2 and JAK3 pathways. This *in vivo* study further demonstrated that CS bioceramics could stimulate osteogenesis better than β-TCP implants by accelerating new bone formation at defective sites in the femur. These findings improve our understanding of immune modulation of CS bioactive ceramics and facilitate strategies to improve the *in vitro* osteogenesis capability of bone substitute materials.

1. Introduction

Bone defects caused by trauma, tumor, and osteomyelitis have prompted the use of bone regeneration biomaterials [1–6]. Biomaterials for the regeneration of bone defects have rapidly developed from pure biological inert materials to materials that can stimulate osteoblast, osteoclast, and other specific cell responses at the molecular level [7]. Therefore, the current principle for designing biomaterials is to stimulate osteogenic differentiation *in vitro* and to then examine the biomaterials *in vivo* models [8]. *In vivo* and *in vitro* experiments often are inconsistent, however, which in turn hinders the clinical application of biomaterials [9]. The contradiction implies that we may focus more on the *in vitro* characteristics of materials but ignore their *in vivo* biological effect [10].

Recently, the development of osteoimmunology has changed our focus on the *in vivo* interactions among host immune cells, bone cells, and biomaterials [8,11]. During fracture healing, osteoblasts and osteoclasts indicate a dynamic balance in bone formation and remodeling [12,13]. Immune cells can produce inflammatory cytokines, including interleukin-1 (IL-1), IL-6, and tumor necrosis factor-α (TNF-α), or can transform cell subtypes to regulate osteoclastogenesis using cytokine macrophage-colony stimulating factor (M-CSF), osteoprotegerin (OPG), and receptor activator of NF-κB ligand (RANKL) [14,15]. Some studies, however, also suggest that immune cells can regulate osteoblasts

Peer review under responsibility of KeAi Communications Co., Ltd.
* Corresponding author.
** Corresponding author.
*** Corresponding author.
E-mail addresses: lklecnu@aliyun.com (K. Lin), shougui126@126.com (S. Xu), liujqmj@163.com (J. Liu).
[1] These authors contributed equally.

https://doi.org/10.1016/j.bioactmat.2020.09.018
Received 19 March 2020; Received in revised form 18 September 2020; Accepted 18 September 2020

through the regulatory molecules, including transforming growth factor-β (TGF-β), IL-10, and vascular endothelial growth factor (VEGF) [16–18]. Correspondingly, "smart" biomaterials, as foreign implants, should be able to induce beneficial immune responses in immune cells, thereby building an osteogenesis-promoting environment for bone cells and enhancing implant integration [19]. Therefore, it is important to explore the functional plasticity of immune cells in biomaterial-induced bone formation.

As innate immune cells, macrophages are among the first cells to act against foreign elements, such as biomaterials, playing an essential role in material-induced immune reactions [20,21]. Characterized by different cytokine secretions and surface markers, macrophages have two major phenotypes, namely, M1 and M2. The biomaterial-induced environment can stimulate macrophages to transform their phenotype and physiological function [22]. Classically, inflammatory macrophages (M1), with the typical surface marker CD11c, are well known to enhance Th1-biased inflammation by pro-inflammatory cytokines (IL-6, TNF-α), which enhance osteoclastic activities [23]. By contrast, alternative anti-inflammatory macrophages (M2), with the typical surface marker CD206, are helpful in enhancing Th2-biased inflammation [24] by anti-inflammatory cytokines, such as IL-10, which is beneficial for the formation of new bones or fibrous capsules [8]; macrophages also secrete a range of osteoinductive molecules, such as BMP-2 and TGF-β, to promote osteogenesis [25,26]. Furthermore, as the precursors of osteoclasts, macrophages participate in the degradation of biomaterial and the remodeling of bone [27]. The diversity and flexibility of macrophages make them a major target for modulating biomaterial-induced immune reactions [28]. Further investigations should be performed to better characterize alternate macrophage phenotypes to understand how host immune cells, bone cells, and biomaterials coordinate.

It has been reported that biomaterials with special components and surface topographies can also induce macrophage polarization, switching from pro-inflammatory M1 to anti-inflammatory M2 types [29]. In addition, the polarization induced by the materials may be closely related to their osteogenic activity. Our previous studies have shown that calcium silicate ($CaSiO_3$, CS)-based biomaterials are more effective for bone marrow mesenchymal stem cell (BMSC) proliferation, osteogenic differentiation, and bone formation compared with the traditional Ca–P based materials [30,31]. However, whether or not the CS bioceramics have osteoimmunomodulatory properties remains unclear.

Herein, we tested the *in vitro* osteogenic capacity of CS in the modulation of macrophages by comparison with the commonly used osteoconductive material β-TCP. By detecting the functional switch of macrophages *in vitro*, we can predict which biomaterials may be better for osteogenesis, as determined by *in vivo* animal experiments. Therefore, the application of osteoimmunology in the design of the bone materials provides us with ideas to evaluate the materials in osteogenesis and to explore the mechanism of material-induced bone healing.

2. Materials and methods

2.1. Preparation and characterization of β-$Ca_3(PO_4)_2$ and $CaSiO_3$ bioceramic particles

β-Tricalcium phosphate (β-$Ca_3(PO_4)_2$, β-TCP) and $CaSiO_3$ (CS) bioceramic particles with a size of 300–450 μm were obtained by the calcining method. First, β-TCP and CS powders were synthetized using chemical precipitation, as described in our previous study [30,32–34]. All reagents were analytical-grade and purchased from China National Medicine Shanghai Chemical Reagent Corporation. For the β-TCP powders, analytical-grade $Ca(NO_3)_2{\cdot}4H_2O$ and $(NH_4)_2HPO_4$ were successively dissolved into aqueous solutions at a concentration of 0.5 M. Then, the $Ca(NO_3)_2$ aqueous solution was dripped into the $(NH_4)_2HPO_4$ aqueous solution under constant stirring until the molar ratio of Ca/P reached 1.5; the pH value of the reaction system was controlled at around 8.0 using ammonium hydroxide. After stirring the precipitates for 24 h after complete addition, the products were filtered and washed with deionized water three times. Then the β-TCP powders was acquired by calcination at 800 °C for 2 h. We utilized the same method for the CS powder preparation, which used $Ca(NO_3)_2{\cdot}4H_2O$ and $CaSiO_3{\cdot}9H_2O$ as raw materials, and set the Ca/Si molar ratio to 1.0.

Each of the obtained β-TCP and CS powders were mixed with 8% (wt) polyvinyl alcohol aqueous solution. Then, we uniaxially compressed the powders into plates with a 25-mm diameter and 10-mm thickness using stainless steel die. The β-TCP and CS biscuits were calcined at 1050 °C for 5 h and subsequently cooled to about 25 °C in the furnace. After calcination, the β-TCP and CS plates were crushed and filtered to obtain particles with a diameter of 300–450 μm.

The phase and morphology of the final products were determined using X-ray diffraction (XRD, Geigerflex, Rigaku Co., Japan) with monochromated CuKα radiation and scanning electron microscopy (SEM: JSM-6700F, JEOL, Japan), respectively.

2.2. Macrophage culture and stimulation using material extracts

2.2.1. Isolation and culture of BMDMs

The isolation and culture of bone marrow-derived macrophages (BMDMs) was conducted as previously described [35]. In detail, femurs and tibias were isolated from C57BL/6 mice (Joint Ventures Sipper BK Experimental Animal, Shanghai, China) within an age range of 6–8 weeks. Each group consisted of six mice, and we the experiments were repeated three times independently. Bone marrow was cleansed with phosphate buffer saline (PBS) using a 1 mL syringe. Then, the cells were forced through a 70 μm cell filter to get rid of cell clumps, 1 mL Tris-NH_4Cl solution was added, and the suspension was incubated for 10 min on ice to discard the red blood cells. The isolated bone marrow cells were resuspended in BMDM growth medium (Dulbecco's modified Eagle medium [DMEM, Invitrogen, Carlsbad, CA, USA] [36] supplemented with 10% fetal bovine serum [FBS, Invitrogen] and 10 ng/mL M-CSF, R&D Systems, Minneapolis, MN, USA) and were then seeded into six-well tissue culture plates. On day 7, the mature BMDM formation by flow cytometry analysis was assessed to detect cells that expressed CD11b and F4/80 (both antibodies were obtained from eBiosciences, San Diego, CA, USA). To increase the purity of the macrophages, the non-adherent cells were washed off before use.

2.2.2. Preparation of the material extracts and stimulation of BMDMs

The material extracts were prepared by soaking CS and β-TCP bioceramic powders in serum-free DMEM in succession at a solid/liquid ratio of 100 mg/mL, respectively. The mixture was first incubated at 37 °C for 24 h and then centrifuged. We collected the supernatant and passed it through 0.2-mm filter membranes for sterilization (Pall Corporation, Port Washington, NY, USA). The levels of endotoxins in the material extracts was measured before use. In the present study, the extract of the β-TCP bioceramics were used, which is traditional bone graft in clinics, as the control sample.

The mature BMDMs were seeded into a 24-well tissue culture plate at a density of 1×10^5 cells/well. After 12 h, the culture medium was replaced with 500 μL of the material extract supplemented with 10% FBS. DMEM containing 10% FBS but without the mineral extract was used as the control sample. The ion concentrations of Ca and Si in cell culture mediums with CS and β-TCP bioceramic extract components were determined by inductively coupled plasma optical emission spectroscopy (ICP-OES; 710-ES, Varian, Palo Alto, CA, USA). The pH values of the cell culture mediums with the bioceramic extract components were determined by using an electrolyte type pH meter (pH-FE28, Five Easy Plus, Shanghai, China). Then, the cells were collected to assess mRNA, protein, and surface marker expression using the following methods. To give a dynamic observation of the gene and protein expression for BMDMs, the mRNA expression of inflammatory factors was detected within 12 h and the mRNA expression of M-CSF, VEGF,

and OSM within 24 h. The protein levels of these factors were detected within 24 h after treatment with CS or the β-TCP extract. After incubation for 48 h, the supernatant was collected as the conditioned medium.

2.2.3. BMSC isolation and stimulation with the conditioned medium

Isolation and cultivation of BMSCs according to protocols established in former studies was performed [9]. Briefly, bone marrow was obtained from the femoral bone marrow cavity of C57BL/6 mice. Density gradient centrifugation was used for the isolation of mononuclear cells from bone marrow with the addition of Lymphoprep. Tissue culture bottles that contained DMEM supplemented with 10% FBS were seeded with the collected cells. The medium was replaced at 3-day intervals until the primary mesenchymal cells reached 80% confluency. Non-adherent hematopoietic cells were discarded with the replaced medium. The BMSCs based on their morphology was characterized as previously described [9]. To stimulate the BMSCs with the conditioned medium, the culture medium (DMEM + 20% FBS) was supplemented with the collected conditioned medium at a ratio of 1:1. The pure material extract and culture medium that were not supplemented with the conditioned medium served as controls. To measure the expression of bone-related genes, including osteopontin (*OPN*), osteocalcin (*OCN*), alkaline phosphatase (*ALP*), and collagen type I (*COL1*), as well as the protein expression of BMSCs, including ALP and OPN, the BMSCs were seeded into 12-well plates at a density of 2×10^5 cells/well. After incubation for 12 h, we substituted the culture medium with conditioned medium or control medium.

2.3. Flow cytometry

For flow cytometry detection of surface makers, macrophages were cultured from isolated bone marrow cells supplemented with 10 ng/mL M-CSF for 7 days. And then, flow cytometry analysis was used to identify macrophage polarization at 2 days after treatment with CS or the β-TCP extract. We incubated the BMDMs with anti-mouse CD16 and anti-mouse CD32 (eBiosciences, San Diego, CA, USA) at 25 °C for 20 min to inhibit the Fc receptor from nonspecific binding. The cells were then washed with PBS and stained with the previously mentioned antibodies at 25 °C for 20 min. We performed all flow cytometric analysis on a fluorescence-activated cell sorter (FACS) LSR Fortessa with FACSDiva software (BD Biosciences, San Jose, CA, USA).

2.4. Quantitative RT-PCR

Quantitative real-time PCR (qRT-PCR) analysis was performed as previously described [37] using a LightCycler and a SYBR RT-PCR kit. Total RNA isolation and purification was performed with an RNeasy Mini Kit (Qiagen, Valencia, CA, USA). Approximately 1 μg of total RNA was used for the synthesis of complementary DNA (cDNA) by the FSQ-201 ReverTra Ace qPCR RT Kit (Toyobo, Osaka, Japan). We conducted RT-PCR analysis with diluted cDNA and SYBR Green Realtime PCR Master Mix (Toyobo, Osaka, Japan) in a LightCycler 1.5 PCR system (Roche, Penzberg, Germany). The mean cycle threshold (Ct) value of each target gene was normalized against the Ct value of a housekeeping gene (*β-actin*) to determine relative expression levels. For the calculation of fold changes, all related genes were normalized to the controls as shown in the first column. We used Primer 3 software (http://bioinfo.ut.ee/primer3-0.4.0) to design the sequences of primers (Table 1).

2.5. Enzyme linked immunosorbent assay (ELISA)

Conditioned medium from BMDMs treated with CS or the β-TCP extract was collected as above. Then, inflammatory factors and OSM was detected using enzyme linked immunosorbent assay (ELISA) kits (R &D Systems, Minneapolis, MN) according to the manufacturer's protocols.

Table 1
Sequences of primers used in this study.

Gene	Primer sequences
β-actin	**F**: 5′-AGTGTGACGTTGACATCCGT-3′ **R**: 5′-GCAGCTCAGTAACAGTCCGC-3′
IL-1β	**F**: 5′-TGCCACCTTTTGACAGTGATG-3′ **R**: 5′-TGATGTGCTGCTGCGAGATT-3′
TNF-α	**F**: 5′-CTGAACTTCGGGGTGATCGG-3′ **R**: 5′-GCTTGTCACTCGAATTTTGAGA-3′
IL-10	**F**: 5′-GCTCTTACTGACTGGCATGAG-3′ **R**: 5′-CGCAGCTCTAGGAGCATGTG-3′
TGF-β1	**F**: 5′-CTCCCGTGGCTTCTAGTGC-3′ **R**: 5′-GCCTTAGTTTGGACAGGATCTG-3′
OSM	**F**: 5′-CCCGGCACAATATCCTCGG-3′ **R**: 5′-TCTGGTGTTGTAGTGGACCGT-3′
VEGF	**F**: 5′-CACATAGAGAGAATGAGCTTC-3′ **R**: 5′-CTCCGCTCTGAACAAGGCT-3′
M-CSF	**F**: 5′-GGCTTGGCTTGGGATGATTCT-3′ **R**: 5′-GAGGGTCTGGCAGGTACTC-3′
OPN	**F**: 5′-TCACCTGTGCCATACCAGTTA-3′ **R**: 5′-TGAGATGGGTCAGGGTTTAGC-3′
OCN	**F**: 5′-GCAAAGGTGCAGCCTTTGTG-3′ **R**: 5′-GGCTCCCAGCCATTGATACAG-3′
ALP	**F**: 5′-TCAGAAGCTAACACCAACG-3′ **R**: 5′-TTGTACGTCTTGGAGAGGGC-3′
COL1	**F**: 5′-AGAACAGCGTGGCCT-3′ **R**: 5′-TCCGGTGTGACTCGT-3′

Table 2
The ion concentration and pH value of the cell culture mediums with CS and β-TCP extracts.

Groups	Ca^{2+} (ppm)	Si^{4+} (ppm)	pH
With β-TCP extract	623.21	2.32	7.81
With CS extract	626.19	10.82	7.87

2.6. Alkaline phosphatase staining and quantification

ALP staining was made using a BCIP/NBT Alkaline Phosphatase Colour Development Kit (Beyotime) on day 10. Washed the cells twice with PBS, then with glutaraldehyde 2.5%, 300 μl/W, fixed for 10min, rinsed twice with PBS, then configured and added BCIP/NBT staining working solution according to the product instructions, next, incubated at room temperature in the dark for 5–30min, removed BCIP/NBT dyeing working solution, at last, washed 1–2 times with water to stop the color reaction. Quantification of ALP staining was done by ImageJ. In detail, ImageJ software was used for quantification of positively stained area. Then, the area of positive staining was divided by total area to make percentage of positively stained area. Finally, the ALP levels were normalized to the “Blank” group.

2.7. In vivo experiments for biomaterials

2.7.1. Animal and surgical procedures

Wistar rats (National Tissue Engineering Center, Shanghai, China) were kept for 2 weeks before the experiments. We conducted experiments in accordance with the NIH Guidelines for Laboratory Animal Care and Use (NIH 85-23 Rev. 1985) and surgical protocols were approved by the Research Center for Laboratory Animal of the Second Military Medical University of China. A total of 60 rats underwent bilateral femur implantations and were divided into two groups: the β-TCP implant group (n = 30; rats underwent surgery, with the defect filled with β-TCP implants) and the CS implant group (n = 30; rats underwent surgery, with the defect filled with CS material). The rats were anesthetized using isoflurane. Approximately 6-mm-long bilateral longitudinal skin incision was made to expose the middle portion of the femurs. Then, 6 × 2 mm artificial femoral bone defects were drilled in the shaft of both femurs using a trephine bur and filled the particle

implants into the drill holes. Subsequently, the soft tissues were closed and sutured the skin. To study bone healing over time, the animals were killed in a CO_2 chamber at 4, 8, and 12 weeks after the operation.

2.7.2. 3D micro-CT imaging

The additional evaluation of femur bone structure was analyzed using a microcomputed tomography (micro-CT) imaging apparatus (GE Explore Locus SP micro-CT, USA). First, the defective femurs were scanned under the following CT parameters: voltage, 80 kV; currency, 124 μA; and resolution, 8 μm. Then, to evaluate the process of bone formation, two-dimensional slice images were used to reconstruct the 3D micro-CT images with Microview 2.2 software (GE Health Systems, Chicago, IL, USA). Moreover, the percentages of new bone volume against total tissue volume (BV/TV) and bone mineral density (BMD) were assessed using auxiliary histomorphometric software (Scanco Medical AG, Switzerland).

2.7.3. Histological and observation

All procedures were performed using previously described methods [38]. The limbs at weeks 4, 8, and 12 were dehydrated in graded alcohol (from 75% to 100%) and embedded in polymethyl methacrylate. An axial section of each specimen was cut and stained by van Gieson's picrofuchsin for the histological observation of new bone formation. The areas of new bone were measured and analyzed using Image Pro version 5.0 analysis software (Media Cybernetic, Silver Springs, MD, USA). Areas of new bone were presented as a percentage of the maximum new bone area value in the experimental data.

2.8. Statistical analysis

All values are expressed as the mean ± standard deviation (SD). The unpaired Student *t*-test was used in data analysis. Statistical significance was defined as $P < 0.05$.

3. Results

3.1. Material characterization of β-TCP and CS, ion concentration and pH of β-TCP and CS extracts

Fig. 1 A confirms that the prepared particles were pure β-$Ca_3(PO_4)_2$ and β-$CaSiO_3$ phases. The SEM images revealed that the prepared β-TCP and CS particles were irregularly shaped, with a size range of 300–450 μm (Fig. 1B). The ion concentration and pH value of the cell culture mediums with β-TCP and CS extract components, respectively were showed in Table 2. There was no difference between the two groups in the concentration of Ca^{2+}. However, the CS has obviously higher silicon (Si) ion content than the β-TCP group. The pH of CS extracts was 7.87 and β-TCP extracts was 7.81, which were both slightly alkaline microenvironment.

3.2. Immunomodulatory properties of material extracts of the macrophages

3.2.1. Polarization of BMDMs with CS extracts

We used the BMDMs to investigate the activation of material extracts on the immunomodulatory properties of macrophages, which were more representative of macrophages in the local microenvironment (Fig. 2A). After induction of bone marrow cells, we confirmed the differentiation into BMDMs was successful by detecting the expression of CD11b and F4/80, the traditional surface markers of macrophages (Fig. 2B). Then, we cultured the BMDMs with material extracts from the CS or β-TCP controls (Fig. 2A).

3.2.2. The M1 and M2 surface markers of BMDMs

We investigated the influence of the material extracts on the classical M1 and M2 markers of macrophages. We used FACS to study the M1 and M2 surface markers of BMDMs after treatment with different material extracts. The M1 surface marker CD11c in BMDMs induced with β-TCP extracts showed a higher fluorescence value compared with the CS treatment group. However, the mean fluorescence intensity of the M2 surface marker of CD206 was significantly lower in the β-TCP group, which indicated a shift from the M1 to M2 type after CS extract treatment (Fig. 3A and B).

3.2.3. Expression of inflammatory cytokines in BMDMs

To further confirm the phenotype switch of BMDMs, we investigated the inflammatory gene expression levels after extract treatment. The mRNA expression of M1 genes, such as *IL-1β* and *TNF-α*, was significantly downregulated in BMDMs treated with the CS extracts ($P < 0.05$) compared with the β-TCP group. However, the expression of M2 genes, such as *IL-10* and *TGF-β*, was significantly upregulated upon treatment with the same stimulants ($P < 0.05$) (Fig. 3C). Consistent with the qRT-PCR results, the secretion of IL-1β, TNF-α, IL-10, and TGF-β as detected by ELISA showed similar trends (Fig. 3D). Thus, CS extract treatment may induce BMDMs to switch phenotypes from M1 to M2.

3.2.4. Effects of BMDM-conditioned medium on the osteogenic differentiation of BMSCs

3.2.4.1. BMDM-conditioned medium treated by CS extract promotes the osteogenic differentiation of BMSCs. Previous studies have reported that the phenotypic switch of macrophages regulates osteogenic differentiation of BMSCs through secreting factors [39]. Thus, we sought to determine whether the conditioned medium of BMDMs treated by material extracts had the same effects. First, we detected the expression of osteogenesis-related genes in BMDMs upon material extract treatment. The M-CSF and VEGF expression showed no difference between the CS and β-TCP extract treatment groups ($P > 0.05$) (Fig. 4A and B). However, the expression of oncostatin M (OSM) was upregulated in response to CS extract treatment (Fig. 4C and D).

Next, we used the conditioned medium of BMDMs to stimulate the BMSCs. The mRNA expression levels of *OPN*, *ALP*, and *COL1*, genes that are relevant to mineralization, were significantly upregulated in BMSCs stimulated by the BMDM-conditioned medium treated by the CS extract, in contrast to that treated by the β-TCP extract ($P < 0.05$) (Fig. 5A, C, and 5D). Western blotting also exhibited a significant increase in the protein expression of OPN and ALP in the CS-treated group (Fig. 6A–C). Direct treatment of BMSCs with both material extracts, however, had a much weaker effect on the expression of these genes. Then, we used ALP staining to evaluate osteogenic differentiation. In staining, the insoluble dark blue to blue-violet precipitate formed by ALP can indirectly reflect the activity of ALP. Obviously, cells treated with the BMDM-conditioned medium treated by CS extracts formed more precipitate than cells treated with medium treated by β-TCP extracts (Fig. 7A–C). These results were confirmed by the quantification analysis of ALP staining by ImageJ (Fig. 7D).

3.2.4.2. Oncostatin M mediates the osteogenic differentiation of BMSCs via the ERK1/2 and JAK3 pathways. Next, we sought to determine the factors in the CS-conditioned medium that mediated the osteogenic differentiation of BMSCs. As the expression of OSM was upregulated in the CS-conditioned medium (Fig. 4C and D), the medium had a weaker effect on ALP and OPN expression in BMSCs than in the controls after silencing of the OSM gene in BMDM (Fig. 8B and C). It has been reported that *OSM* can promote osteogenesis via the ERK1/2 and JAK3 pathways [40]. To determine the mechanism underlying the osteogenic differentiation of BMSCs, we detected the involved pathway upon BMDM-conditioned medium treatment. Fig. 8E and F shows that ERK1/2 and JAK3 were upregulated in BMSCs stimulated by the BMDM-conditioned medium treated with the CS extract, which can be reversed by silencing the *OSM* gene in BMDM. Direct treatment of BMSCs with CS extracts, however, did not impart the same effect

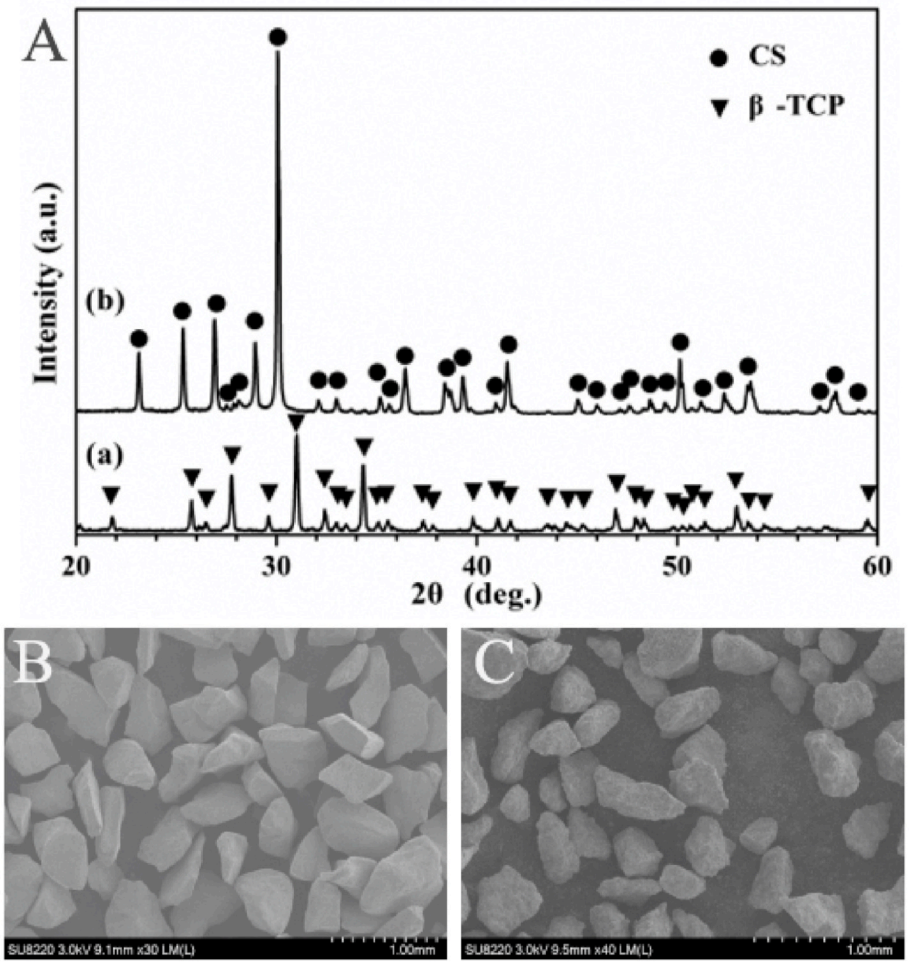

Fig. 1. (A) XRD patterns of the β-TCP and CS particles. (B) and (C) SEM morphologies of (B) β-TCP and (C) CS particles, respectively.

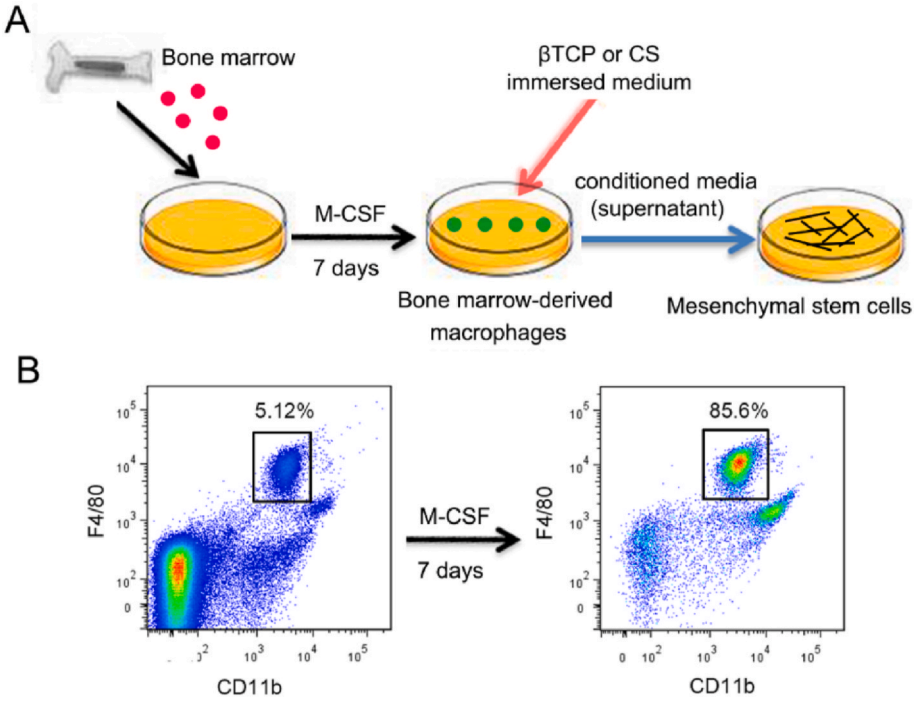

Fig. 2. Schematic illustration of the experiment. (A) Schematic illustration of the culture of BMDMs and the stimulation of BMDMs and BMSCs. (B) FACS analysis of CD11b and F4/80 expression in BMDMs with or without M-CSF induction.

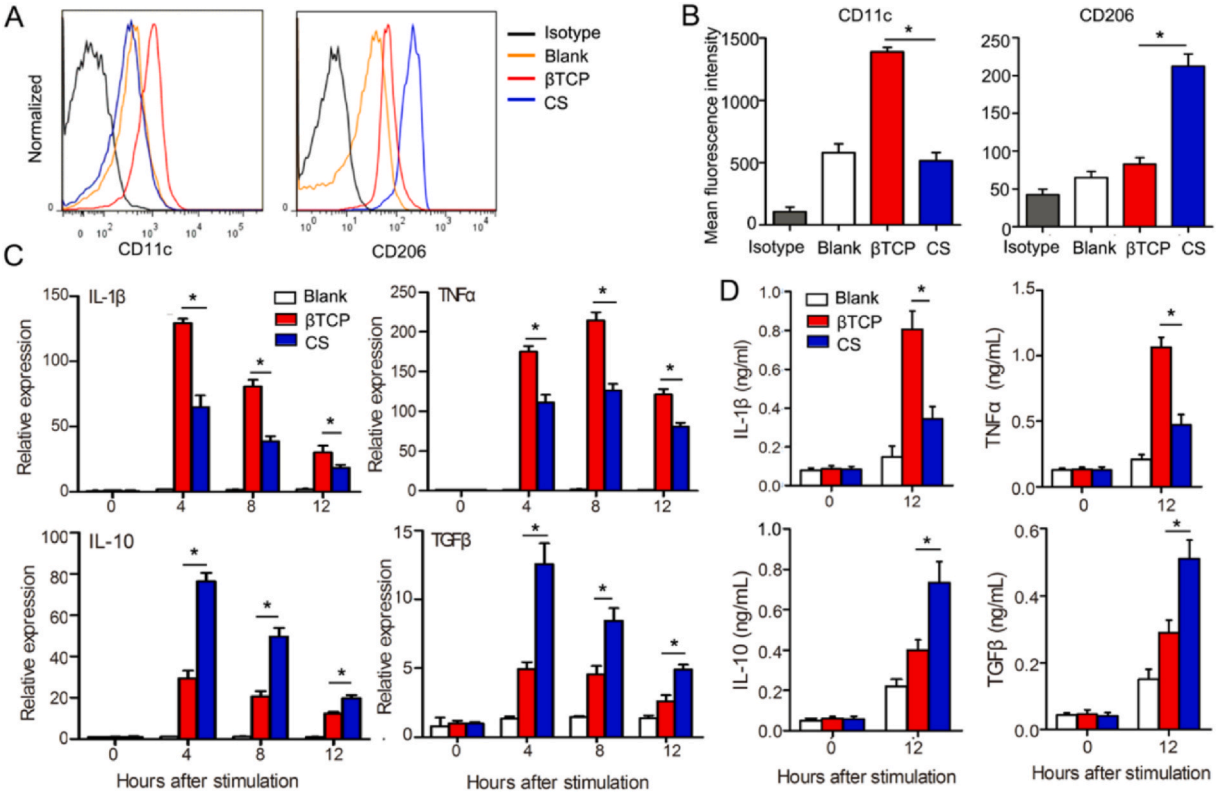

Fig. 3. CS extracts promote the polarization of BMDMs. (A) FACS analysis and (B) quantification of mean fluorescence intensity for CD11c and CD206 expression of BMDMs treated with CS or the β-TCP extract. (C) mRNA expression levels of *IL-1β*, *TNF-α*, *IL-10*, and *TGF-β* relative to *β-actin* in BMDMs with the stimulation of CS and β-TCP extract for 0, 4, 8, and 12 h. (D) Protein expression levels of IL-1β, TNF-α, IL-10, and TGF-β were determined by ELISA. *$P < 0.05$. The result was normalized to "Blank."

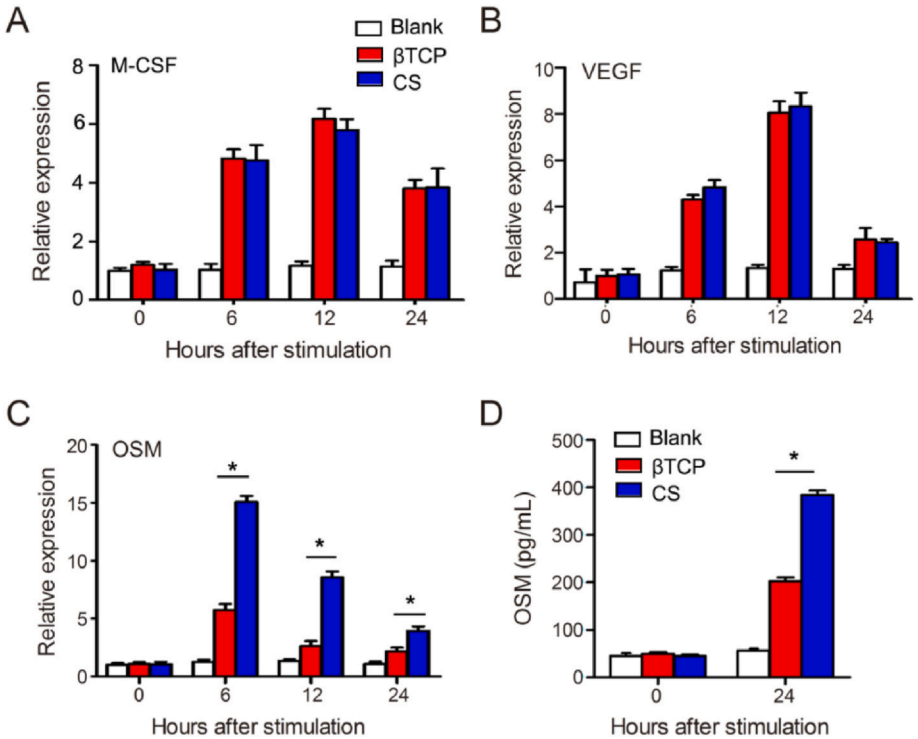

Fig. 4. mRNA expression levels of (A) *M-CSF*, (B) *VEGF*, and (C) *OSM* relative to *β-actin* by BMDMs with the stimulation of CS and β-TCP extract (conditioned medium) for 0, 6, 12, and 24 h. (D) OSM protein expression levels were determined by ELISA. *$P < 0.05$. The result was normalized to "Blank."

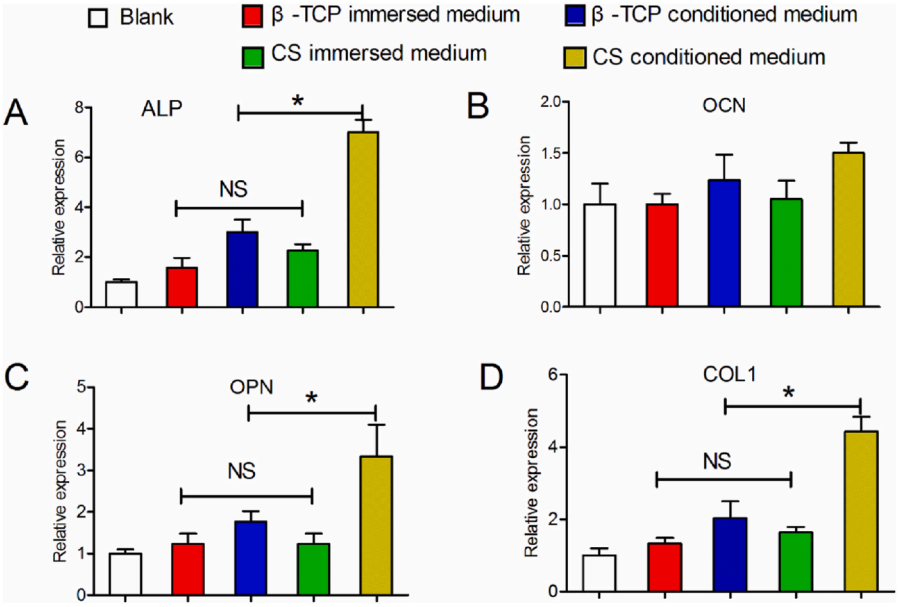

Fig. 5. mRNA expression levels of (A) *ALP*, (B) *OCN*, (C) *OPN*, and (D) *COL1* relative to *β-actin* in BMSCs stimulated by the CS extract, β-TCP extract, or BMDM-conditioned medium treated with these two extracts. *$P < 0.05$, "NS" represents "not significant." The result was normalized to "Blank."

(Fig. 8D–F). On the basis of these results, OSM can promote the osteogenic differentiation of BMSCs through the ERK1/2 and JAK3 pathways. The same trend was found at the protein level (Fig. 8D–F).

3.3. In vivo osteoimmunology modulation of bone formation

To compare the osteogenic properties of the two materials *in vivo*, we used micro-CT and tissue sections for evaluation in the animal experiments. The micro-CT scanning exhibited different patterns of new bone formation between the β-TCP implant and CS implant groups compared with the sham group 4, 8, and 12 weeks after implantation (Fig. 9A). We observed enhanced new bone formation in the CS implant group compared with the β-TCP implant group ($P < 0.05$). As detected in the following morphometric analysis: BMD in the CS implant group was greater than that in the β-TCP implant group (Fig. 9B). The β-TCP implant and CS implant groups both showed a significantly higher percentage of BV/TV, in contrast, with respect to the CS implant and the β-TCP implant groups, the former group showed a higher percentage of BT/VT (Fig. 9C). We detected the same trend in the histological images, in the van Gieson's picrofuchsin histological observation, both

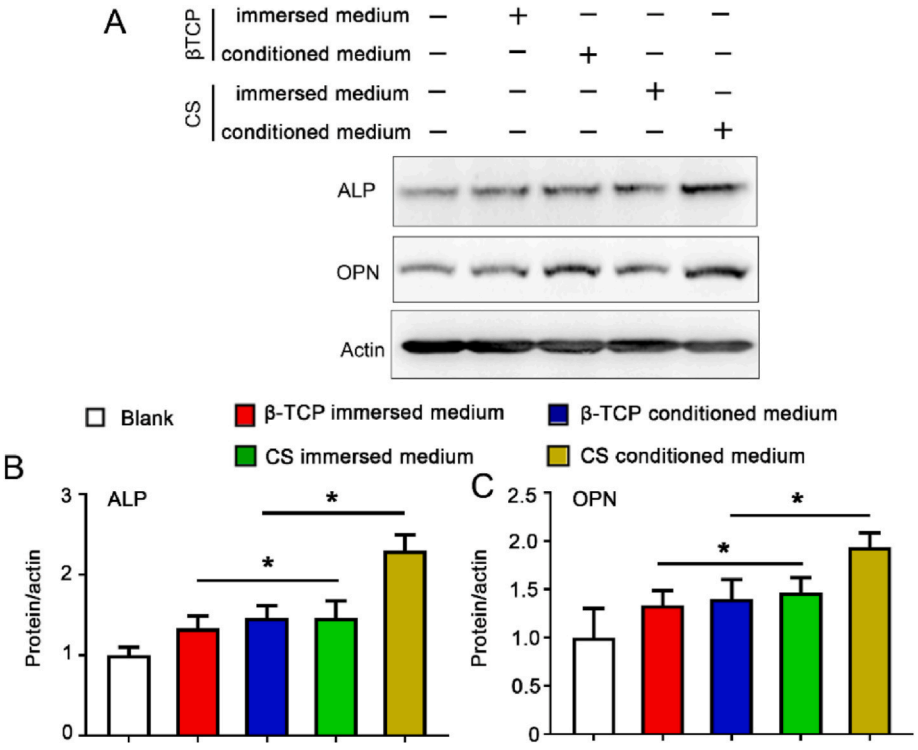

Fig. 6. (A) Protein levels and (B and C) quantification results of ALP and OPN, as determined by immunoblotting. β-actin was used as a control. *$P < 0.05$, "NS" represents "not significant." The result was normalized to "Blank."

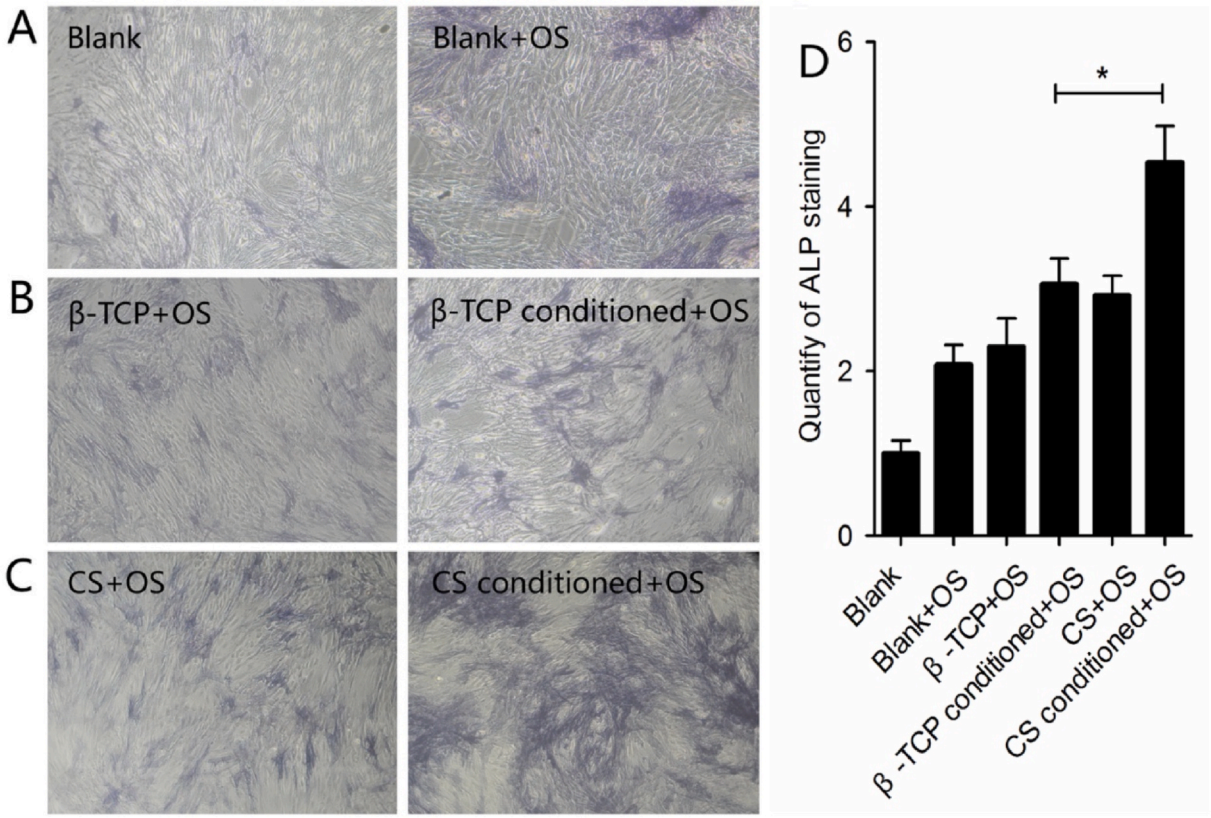

Fig. 7. ALP staining results. (A) BMSCs cultured in cultured medium and with osteogenic supplement (OS). (B) BMSCs cultured in BMDM-conditioned medium treated with the β-TCP extract and with OS. (C) BMSCs cultured in BMDM-conditioned medium treated with the CS extract and with OS. (D) Quantification of ALP staining by ImageJ. The result was normalized to "Blank."

implants were loose in microstructure and spaces between partials were hundreds of micrometers. What's more, the percentage of new bone area in the CS group was higher than in the β-TCP group (Fig. 10A and B).

4. Discussion

Ideal implant materials should stimulate osteogenic differentiation and induce a beneficial osteogenic microenvironment *in vivo;* in particular, these materials should have osteoimmunomodulatory properties. In this study, we found that CS bioceramics could stimulate macrophage polarization and then promote the osteogenic differentiation of BMSCs through OSM in macrophage-conditioned medium through the ERK1/2 and JAK3 pathways.

This study presented strong evidence for the effect of macrophage polarization in biomaterial-mediated osteogenesis. Macrophages can switch their phenotypes between the M1 and M2 extremes in response to environmental changes [41]. We divided the process of *de novo* bone formation into three phases: the early phase, the bone formation phase, and the bone-remodeling phase. The early phase was dominated by the inflammatory phase, in which most of the macrophages were of the inflammatory M1 type. Prolonged M1 extremes led to the formation of a fibro-capsule, resulting in the failure of the new bone formation. At this moment, the efficient switch from the M1 to the M2 phenotype resulted in osteogenic cytokine release and the formation of new bone tissue [8]. In our study, rather than achieving macrophage-mediated osteoimmunity using the macrophage cell line "RAW" or peritoneal macrophages, we used naive macrophages isolated from bone marrow, which resembled the physiological conditions much more closely and were more sensitive to the local microenvironment. Stimulated by the CS extract, macrophages exhibited an elevation in the expression of CD206, which was an M2 surface marker, as well as IL-10 and TGF-β, which were anti-inflammatory cytokines (Fig. 3A–D). In comparison, macrophages exposed to the control material β-TCP exhibited higher expression of CD11c, an M1 surface marker, along with IL-1β and TNF-α, which were pro-inflammatory cytokines (Fig. 3A–D). These findings indicated that CS could induce macrophage differentiation toward the M2 type, whereas the control β-TCP tended to cause a shift toward the M1 type. Previous studies have reported that M1 macrophages secreted various pro-inflammatory cytokines to induce osteoclastogenesis and enhance osteoclastic activities, leading to bone resorption [8]. Besides, at the early stage, after implantation, scaffolds and their degradation materials could activate macrophages [42], which could infer the degradation of CS stimulate immune response and polarize to M2. Thus, our study indicated that CS was more suitable and compatible than β-TCP by preventing pro-inflammatory immune responses to implants, which was beneficial for osteogenesis.

Osteogenesis is the process of apatite formation which has been suggested to be a direct result of the surface reaction of CS *in vitro* and *in vivo*. The dissolution of CS and ion exchanges for hydrogen (pH) play key role among the reaction [36,43]. The immune environment was modulated by CS and contained both bioactive ions released by cell-mediated degradation and chemically dissolved ions. CS was able to adjust the rate of physiological release of Si ions. In the present study, ICP-OES showed that the Si ion concentration in the cell culture medium with CS extract was about 10.82 ppm, whereas Si ion concentration in the cell culture medium with β-TCP extract were 2.32 ppm. At the cellular level, it has Si-containing ionic products could improve the proliferation and osteogenic differentiation of BMSCs and periodontal ligament cells by stimulating the expression of osteogenesis-related genes and bone matrix proteins of BMSCs [44]. Si also was shown to have antioxidant and anti-inflammatory properties, which

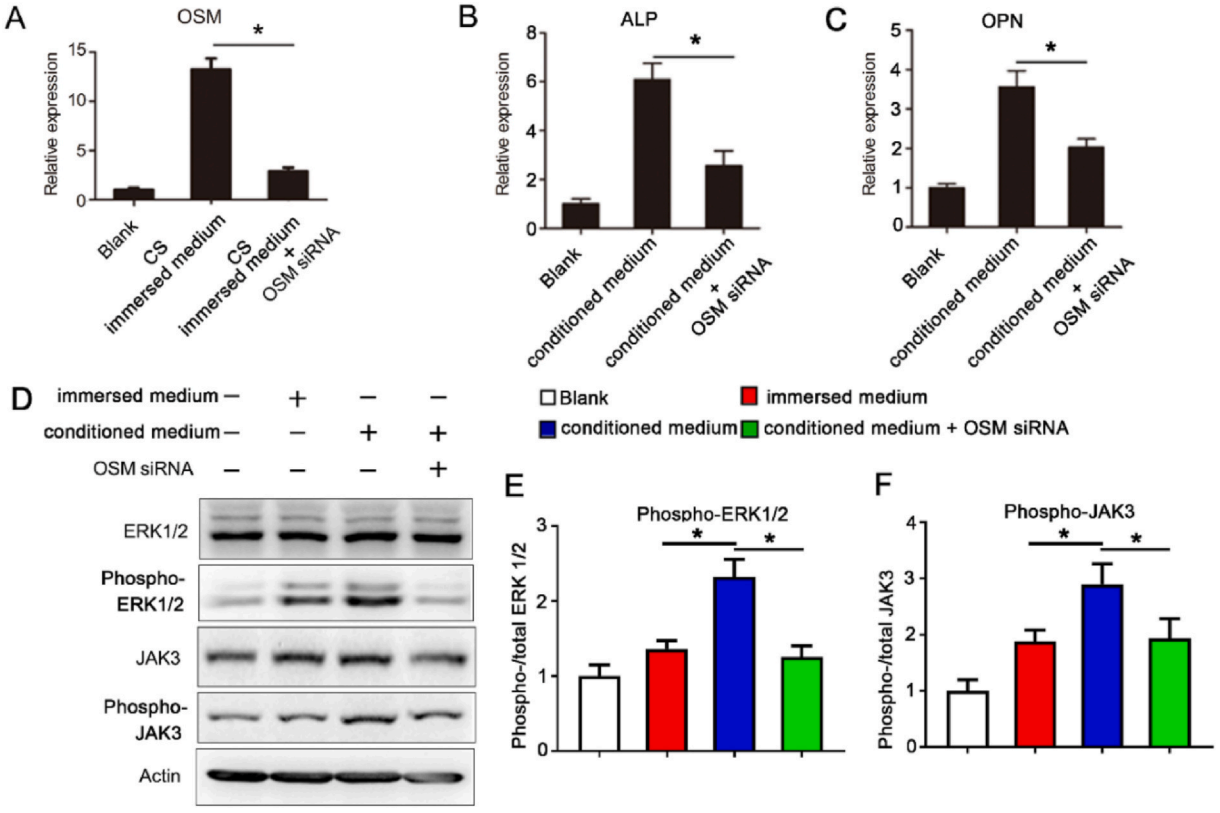

Fig. 8. (A) mRNA expression levels of *OSM* relative to *β-actin* in BMDMs stimulated by the CS extract with or without silencing of OSM. (B and C) mRNA expression levels of *ALP* and *OPN* relative to *β-actin* in BMSCs stimulated by the CS-conditioned medium with or without silencing of OSM. (D) Protein levels and quantification (E and F) results of ERK1/2 and JAK3 and related phosphorylation, as determined by immunoblotting. β-actin was used as a control. Images are shown of one representative experiment. Quantification data are presented as the mean ± SD of three independent experiments. *$P < 0.05$.

were significant in bone metabolism by suppressing the gene expression of inflammatory factors, including *COX-2*, *iNOS*, and *TNF-α* [45]. Lin et al. designed novel Si-substituted hydroxyapatite (Si-HA) nanorods that promoted the osseointegration and biosealing with soft tissue by releasing Si ions [46]. In addition, Si can promote osteoblast activity and bone mineralization by increasing the expression of type I collagen [47], and Si-containing ionic products generated from bioactive glass, coatings, and bioceramics have a similar promoting effect on osteoblasts [48]. It was noted that there was no difference between the two groups in the concentration of Ca^{2+}. However, the CS has obviously higher silicon (Si) ion content than the β-TCP group. Higher concentrations of Si can suppress osteoclasts and their capacity to resorb bone [46], Besides, it has been confirmed that the release of the Si ions could activate the osteogenic genes of osteoblast such as BMP-2, which was an important stimulator of osteogenesis, and up-regulate osteoblast proliferation [49,50]. Although, the β-TCP group has the concentration of 2.32, it may relate to the cell culture medium DMEM, rather than β-TCP, for the normal DMEM also have the silicon (Si) ion component [51]. In conclusion, we could infer the better osteogenesis of CS may related to the higher concentrations of Si. The pH of CS extracts was 7.87 and β-TCP extracts was 7.81. It has been found that the alkaline microenvironment pH is good for bone formation [52,53]. Therefore, both biomaterials could benefit the bone regeneration and the CS was better.

For a greater understanding of the possible mechanism underlying the effect of CS on osteogenesis, we measured the expression of osteogenic genes and proteins in BMDMs. Although the osteogenesis-related *M-CSF* and angiogenesis-related *VEGF* showed no difference, the expression of *OSM* in the macrophages treated by CS was higher than in those treated by β-TCP (Fig. 4A–C). Furthermore, the BMDM-conditioned medium was much more effective than the simple material extract, which indicated that the BMDM-conditioned medium treated with the CS extract enhanced osteogenic differentiation of BMSCs. IL-10 and TGF-β were also released by macrophages stimulated with CS extracts. We did not fully exclude the role of IL-10 and TGF-β. The expression of mineralization-related genes *ALP* and *OPN*, however, was significantly downregulated in BMSCs after silencing of the *OSM* gene in BMDMs, indicating that OSM played a role in the osteogenic differentiation of BMSCs.

OSM, an inflammatory cytokine generally produced by osteoclasts, has attracted increasing attention in the field of osteoimmunity because of its dual effects, as it stimulates both osteogenesis and osteoclastogenesis [54]. *OSM* could directly act on osteoclast precursors or stromal cells to exert osteoclast activity by the upregulation of RANKL, which regulated osteoclastogenesis [55]. The supposed mechanism is that *OSM* could enter the lacunar-canalicular network, which was closest to where resorption takes place, and served as a receptor of osteocytes. Hirata et al. [56], however, demonstrated that ALP activity and mineralization could be strongly induced by *OSM*, which could also be observed in terms of the mRNA and protein expression of ALP in the CS-conditioned medium (Figs. 5A and 6A-B). ALP is closely related to bone calcification [57], which was further confirmed by our ALP staining results (Fig. 7). In cultured BMSCs, *OSM* has also been reported to have synergistic effects with BMP-2 [58]. BMP-2 is a widely recognized osteoinductive agent that can be upregulated by the stimulation of M2 macrophages, which was consistent with our study on the effect of CS-induced M2 extremity.

Although some studies uncovered the role of *OSM* in promoting bone formation by stem cells through the activation of macrophages [59], our study, as a material-based research, focused on the mechanisms and challenges associated with the clinical application of materials, especially the relationship among biomaterials, immune cells, and

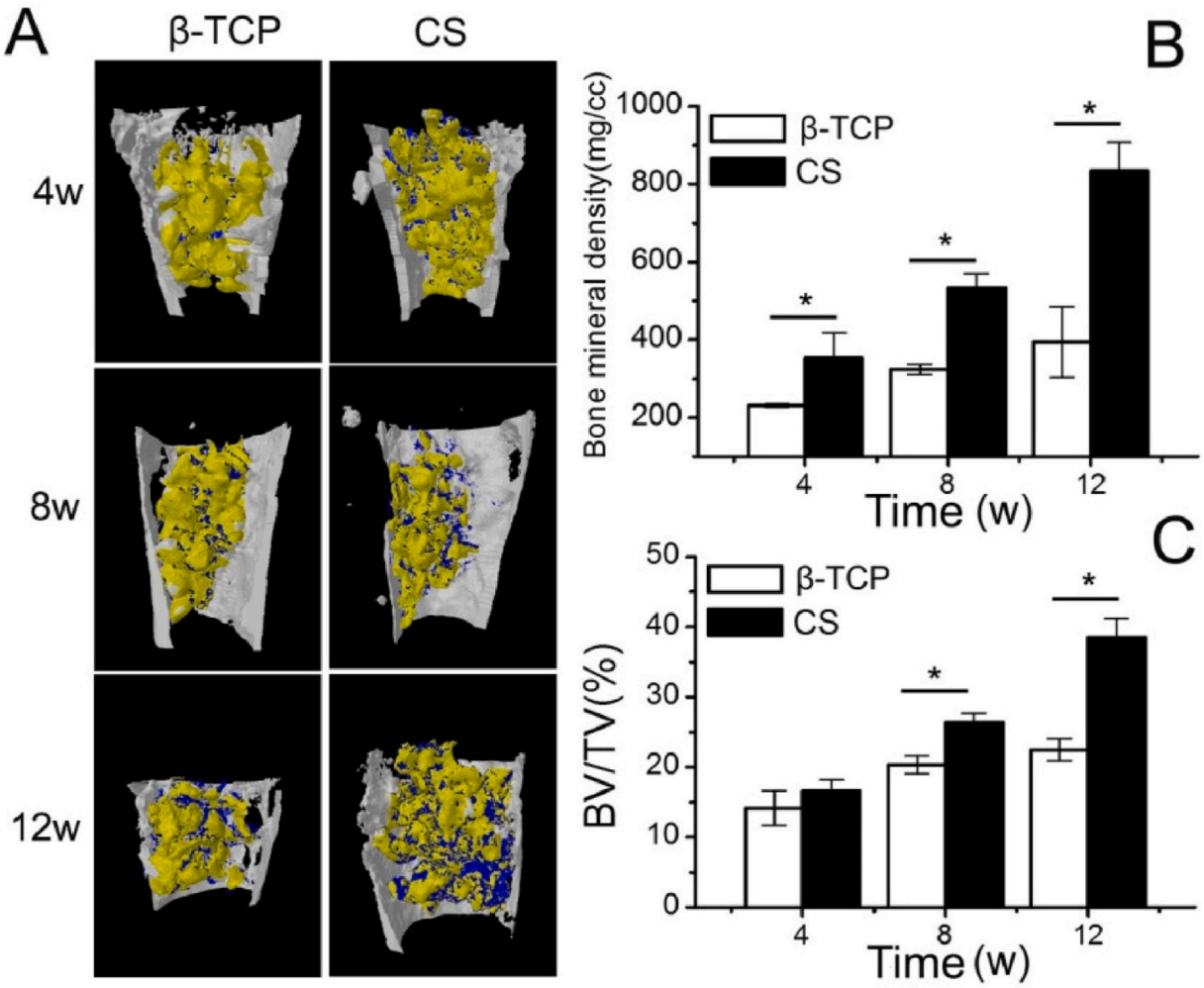

Fig. 9. (A) Coronal section of 3D micro-CT reconstruction of bone regeneration in the femoral bone defect in animals with new bone formation; original bone is shown in white, new bone is shown in yellow, implanted material is shown in blue. (B) The defect sites were analyzed to calculate the BMD. (C) Percentage of new bone relative to total tissue volume (BV/TV) ($n = 10$ rats/batch). *$P < 0.05$. (For interpretation of the references to color in this figure legend, the reader is referred to the Web version of this article.)

bone cells. A previous study verified that CS promoted osteogenesis, and the relationship between osteogenesis and bone formation was examined by measuring the expression of BMP-2 [60]. Mechanistically, it is believed that osteogenesis is promoted by BMP-2 osteogenic protein secreted by macrophages. This study did not delve into the relationship among macrophage subtypes, inflammation, and osteogenesis in sufficient detail to reveal the mechanisms underlying osteoimmunology. Studies to confirm the role of biomaterials *in vivo* have been lacking. Therefore, our research focused mainly on the relationship between biomaterials, host immune cells, and osteogenesis based on clinical issues.

In the mechanism studies, we observed that ERK1/2 and JAK3 were upregulated in BMSCs stimulated by the BMDM-conditioned medium treated with the CS extract, which was reversed by silencing the *OSM* gene in BMDMs (Fig. 8D–F). In addition, cytokines produced by macrophages as a result of CS stimulation played an active role in bone formation, possibly through the activation of the *OSM* pathway. Further experiments on osteogenesis-related genes (*OPN*, *ALP*, and *COL1*) of BMSCs cultured in the CS-conditioned medium revealed much higher expression than in BMSCs cultured in the β-TCP-conditioned medium (Fig. 5A, AC, and AD). The contrast between the two media was also demonstrated by the mineralization level and degree of osteoblast differentiation, which is determined by ALP staining (Fig. 7A–C). All these data strongly indicated that the CS-conditioned medium promoted the osteogenic differentiation of BMSCs by activating the OSM and relevant pathways. We did not fully exclude the role of IL-10 and TGF-β, which were also released by macrophages stimulated with CS extracts. Therefore, future studies need to examine other relevant pathways.

Further investigation also should be conducted to elucidate the role of different macrophage phenotypes on bone formation. Consensus on which macrophage phenotype is more favorable for osteogenesis has not been reached [61], which may be related to the subpopulations of M2 macrophages. M2a macrophages, also known as alternatively activated macrophages, are polarized by the stimulation of IL-10 and IL-4, which boost the secretion of extracellular matrix proteins and collagen, an indispensable process for wound recovery [62]. M2b macrophages are activated by immune complexes and agonists of Toll-like receptor (TLR) [63]. Macrophages recognize the foreign agents through the TLR pathway, which is similar to the mechanisms by which M1 macrophages induce the immune response to degrade or expel the foreign bodies. M2c refers to macrophages activated by IL-10 or glucocorticoid hormones, which regulate immune responses in new bone formation [64]. Therefore, the role of different subpopulations of M2 macrophages and the switch of M1 macrophages in osteogenesis require further investigation. Besides the *in vitro* study, the osteogenesis of two biomaterials has been further evaluated in animals by micro-CT and histological methods, which also confirmed the CS had better osteogenic properties than β-TCP (Figs. 9 and 10). What's more, as the hard

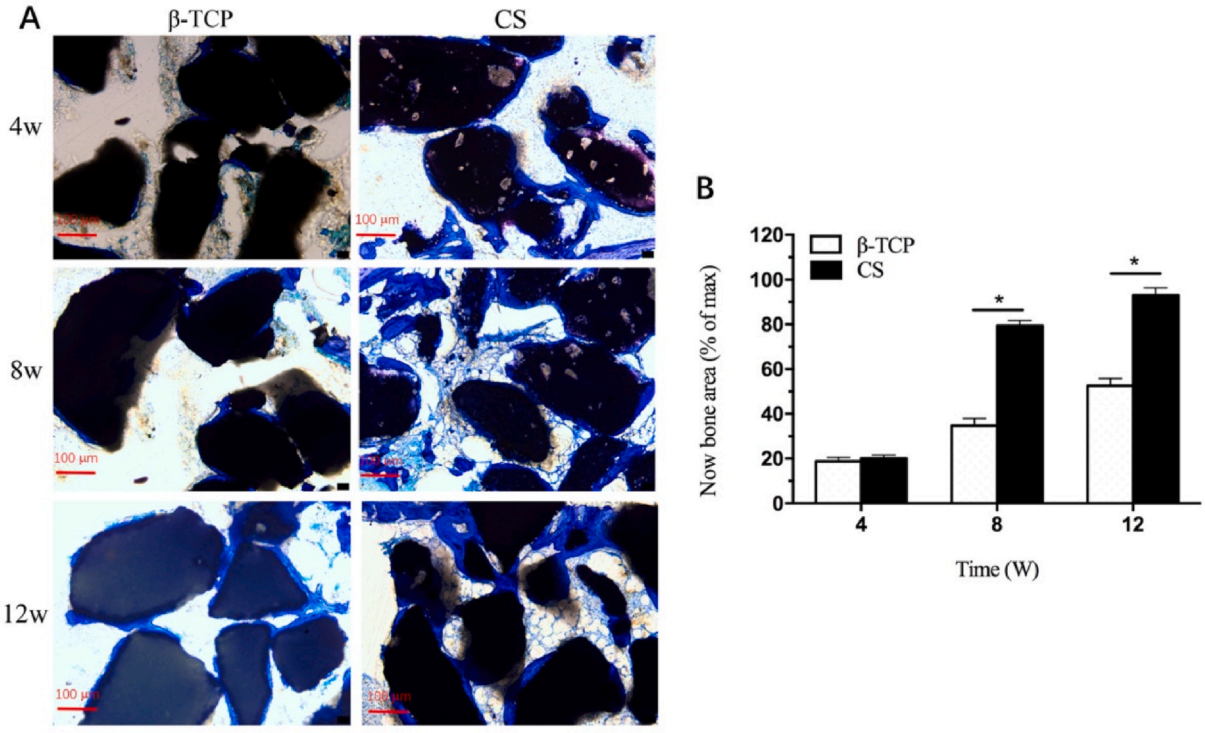

Fig. 10. (A) Histological images of newly formed bone in the femoral bone defect at 4, 8, and 12 weeks after operation; the implants materials are shown in black, the newly formed bone tissues are shown in blue. (B) The percentage of new bone area assessed at 4, 8, and 12 weeks after implantation by histomorphometric analysis. We normalized all new bone area data to the percentage of maximum new bone area value. *$P < 0.05$. (For interpretation of the references to color in this figure legend, the reader is referred to the Web version of this article.)

tissue repair implants, good degradability also need to consider, CS ceramics could stimulate bone regeneration with good bioactive and biodegradable materials has been reported by previous study [65], which was also confirmed in our study that the loose microstructure and appropriate space in Fig. 10. To better evaluate biomaterials in the clinic, further studies are needed to investigate the *in vivo* osteoimmunomodulatory function of the biomaterials. The real immune response induced by biomaterials includes a series of reactions and different types of cells at various stages of new bone formation. It is of great importance to circumvent the technical limitations and to explore complex and dynamic immune responses *in vivo*, which could better promote the applications of biomaterials in the clinic.

5. Conclusions

In conclusion, we demonstrated the manipulation of osteoimmunomodulatory properties of bioactive CS ($CaSiO_3$) bioceramics. Compared with the traditional clinically used β-TCP bioceramics, CS had significantly greater osteoinductive capacity, which was observed both *in vitro* and *in vivo* in the present study. According to our study, CS extract promoted macrophage polarization, thus reducing the host-to-material inflammatory response. Moreover, after stimulation by macrophage-conditioned medium pretreated by CS extracts, the osteogenic differentiation of BMSCs was greatly enhanced by macrophage-derived OSM. These findings confirmed that the participation of macrophages in modulating osteogenesis of bone substitute materials. Therefore, research on the interaction with immune cells, such as macrophages, can be a valuable strategy for evaluating the osteogenic capacity of bone substitute biomaterials.

Declaration of competing interest

The authors have no competing financial interests to declare.

Acknowledgments

The National Natural Science Foundation of China (81571887, 81601910, 81670958, 81701020), Shanghai Rising-Star Program (18QA1405400), Military Medical Research Foundation from the Secondary Military Medical University (2017JS15), Military Medical Science Youth Cultivation Program Incubation Project (No. 20QNPY036), Science and Technology Commission of Shanghai Municipality (19441902900).

References

[1] E.H. Cho, R.L. Shammas, M.J. Carney, J.M. Weissler, A.R. Bauder, A.D. Glener, et al., Muscle versus Fasciocutaneous free flaps in lower extremity traumatic reconstruction: a multicenter outcomes analysis, Plast. Reconstr. Surg. 141 (2018) 191–199, https://doi.org/10.1097/PRS.0000000000003927.
[2] Y. Lu, L. Li, Y. Zhu, X. Wang, M. Li, Z. Lin, et al., Multifunctional copper-containing carboxymethyl chitosan/alginate scaffolds for eradicating clinical bacterial infection and promoting bone formation, ACS Appl. Mater. Interfaces 10 (2018) 127–138, https://doi.org/10.1021/acsami.7b13750.
[3] U. Ritz, R. Gerke, H. Gotz, S. Stein, P.M. Rommens, A new bone substitute developed from 3D-prints of polylactide (PLA) loaded with collagen I: an in vitro study, Int. J. Mol. Sci. 18 (2017), https://doi.org/10.3390/ijms18122569.
[4] C. Zhang, B. Zeng, K. Zhu, L. Zhang, J. Hu, Limb salvage for malignant bone tumours of distal tibia with dual ipsilateral vascularized autogenous fibular graft in a trapezoid-shaped array with ankle arthrodesis and preserving subtalar joint, Foot Ankle Surg. (2017) 278–285, https://doi.org/10.1016/j.fas.2017.11.006.
[5] J.A. Inzana, E.M. Schwarz, S.L. Kates, H.A. Awad, Biomaterials approaches to treating implant-associated osteomyelitis, Biomaterials 81 (2016) 58–71, https://doi.org/10.1016/j.biomaterials.2015.12.012.
[6] W. Wang, K.W.K. Yeung, Bone grafts and biomaterials substitutes for bone defect repair: a review, Bioact Mater 2 (2017) 224–247, https://doi.org/10.1016/j.bioactmat.2017.05.007.
[7] M. Navarro, A. Michiardi, O. Castano, J.A. Planell, Biomaterials in orthopaedics, J. R. Soc. Interface 5 (2008) 1137–1158, https://doi.org/10.1098/rsif.2008.0151.
[8] Z. Chen, T. Klein, R.Z. Murray, R. Crawford, J. Chang, C. Wu, et al., Osteoimmunomodulation for the development of advanced bone biomaterials, Mater. Today 19 (2016) 304–321, https://doi.org/10.1016/j.mattod.2015.11.004.
[9] Z. Chen, C. Wu, W. Gu, T. Klein, R. Crawford, Y. Xiao, Osteogenic differentiation of bone marrow MSCs by β-tricalcium phosphate stimulating macrophages via BMP2

signalling pathway, Biomaterials 35 (2014) 1507–1518, https://doi.org/10.1016/j.biomaterials.2013.11.014.
[10] J.J. Li, M. Ebied, J. Xu, H. Zreiqat, Current approaches to bone tissue engineering: the interface between biology and engineering, Adv. Healthcare Mater. 7 (2017) 1701061.
[11] S. Cheng, D. Zhang, M. Li, X. Liu, Y. Zhang, S. Qian, et al., Osteogenesis, angiogenesis and immune response of Mg-Al layered double hydroxide coating on pure Mg, Bioact. Mater. 6 (2021) 91–105, https://doi.org/10.1016/j.bioactmat.2020.07.014.
[12] Z. Chen, J. Yuen, R. Crawford, J. Chang, C. Wu, Y. Xiao, The effect of osteoimmunomodulation on the osteogenic effects of cobalt incorporated beta-tricalcium phosphate, Biomaterials 61 (2015) 126–138, https://doi.org/10.1016/j.biomaterials.2015.04.044.
[13] D. Zhang, X. Wu, J. Chen, K. Lin, The development of collagen based composite scaffolds for bone regeneration, Bioact Mater 3 (2018) 129–138, https://doi.org/10.1016/j.bioactmat.2017.08.004.
[14] M. Yamashita, F. Otsuka, T. Mukai, R. Yamanaka, H. Otani, Y. Matsumoto, et al., Simvastatin inhibits osteoclast differentiation induced by bone morphogenetic protein-2 and RANKL through regulating MAPK, AKT and Src signaling, Regul. Pept. 162 (2010) 99–108, https://doi.org/10.1016/j.regpep.2010.03.003.
[15] K. Okamoto, T. Nakashima, M. Shinohara, T. Negishikoga, N. Komatsu, A. Terashima, et al., Osteoimmunology: the conceptual framework unifying the immune and skeletal systems, Physiol. Rev. 97 (2017) 1295, https://doi.org/10.1152/physrev.00036.2016.
[16] E. Stavroulaki, M.C. Kastrinaki, C. Pontikoglou, D. Eliopoulos, A. Damianaki, I. Mavroudi, et al., Mesenchymal stem cells contribute to the abnormal bone marrow microenvironment in patients with chronic idiopathic neutropenia by overproduction of transforming growth factor-β1, Stem Cell. Dev. 20 (2011) 1309, https://doi.org/10.1089/scd.2010.0425.
[17] E.J. Chung, K.B. Chien, B.A. Aguado, R.N. Shah, Osteogenic potential of BMP-2-releasing self-assembled membranes, Tissue Eng. A 19 (2013) 2664–2673, https://doi.org/10.1089/ten.tea.2012.0667.
[18] W. Jing, L. Dan, G. Bo, Y. Xiao, X. Chen, X. Zhu, et al., Role of biphasic calcium phosphate ceramic-mediated secretion of signaling molecules by macrophages in migration and osteoblastic differentiation of MSCs, Acta Biomater. 51 (2017) 447–460, https://doi.org/10.1016/j.actbio.2017.01.059.
[19] F. S, S. Rammelt, D. Scharnweber, J.C. Simon, Immune responses to implants - a review of the implications for the design of immunomodulatory biomaterials, Biomaterials 32 (2011) 6692–6709, https://doi.org/10.1016/j.biomaterials.2011.05.078.
[20] M. Shi, Z. Chen, S. Farnaghi, T. Friis, X. Mao, Y. Xiao, et al., Copper-doped mesoporous silica nanospheres, a promising immunomodulatory agent for inducing osteogenesis, Acta Biomater. 30 (2016) 334–344, https://doi.org/10.1016/j.actbio.2015.11.033.
[21] T. Nt, C. Ej, Peptide-based targeting of immunosuppressive cells in cancer, Bioact. Mater. 5 (2020) 92–101, https://doi.org/10.1016/j.bioactmat.2020.01.006.
[22] A. Mantovani, S.K. Biswas, M.R. Galdiero, A. Sica, M. Locati, Macrophage plasticity and polarization in tissue repair and remodelling, J. Pathol. 229 (2013) 176–185, https://doi.org/10.1002/path.4133.
[23] B.N. Brown, J.E. Valentin, A.M. Stewart-Akers, G.P. Mccabe, S.F. Badylak, Macrophage phenotype and remodeling outcomes in response to biologic scaffolds with and without a cellular component, Biomaterials 30 (2009) 1482, https://doi.org/10.1016/j.biomaterials.2008.11.040.
[24] B.N. Brown, R. Londono, S. Tottey, L. Zhang, K.A. Kukla, M.T. Wolf, et al., Macrophage phenotype as a predictor of constructive remodeling following the implantation of biologically derived surgical mesh materials, Acta Biomater. 8 (2012) 978–987, https://doi.org/10.1016/j.actbio.2011.11.031.
[25] Y. Honda, T. Anada, S. Kamakura, M. Nakamura, S. Sugawara, O. Suzuki, Elevated extracellular calcium stimulates secretion of bone morphogenetic protein 2 by a macrophage cell line, Biochem. Biophys. Res. Commun. 345 (2006) 1155–1160, https://doi.org/10.1016/j.bbrc.2006.05.013.
[26] S.M. Wahl, N. Mccartney-Francis, J.B. Allen, E.B. Dougherty, S.F. Dougherty, Macrophage production of TGF-beta and regulation by TGF-beta, Ann. N. Y. Acad. Sci. 593 (1990) 188, https://doi.org/10.1111/j.1749-6632.1990.tb16111.x.
[27] A.R. Pettit, M.K. Chang, D.A. Hume, L.J. Raggatt, Osteal macrophages: a new twist on coupling during bone dynamics, Bone 43 (2008) 976, https://doi.org/10.1016/j.bone.2008.08.128.
[28] B.N. Brown, B.D. Ratner, S.B. Goodman, S. Amar, S.F. Badylak, Macrophage polarization: an opportunity for improved outcomes in biomaterials and regenerative medicine, Biomaterials 33 (2012) 3792–3802, https://doi.org/10.1016/j.biomaterials.2012.02.034.
[29] O.R. Mahon, D.C. Browe, T. Gonzalez-Fernandez, P. Pitacco, I.T. Whelan, S. Von Euw, et al., Nano-particle mediated M2 macrophage polarization enhances bone formation and MSC osteogenesis in an IL-10 dependent manner, Biomaterials 239 (2020) 119833, https://doi.org/10.1016/j.biomaterials.2020.119833.
[30] K. Lin, Y. Liu, H. Huang, L. Chen, Z. Wang, J. Chang, Degradation and silicon excretion of the calcium silicate bioactive ceramics during bone regeneration using rabbit femur defect model, J. Mater. Sci. Mater. Med. 26 (2015) 197, https://doi.org/10.1007/s10856-015-5523-2.
[31] C. Wang, Y. Xue, K. Lin, J. Lu, J. Chang, J. Sun, The enhancement of bone regeneration by a combination of osteoconductivity and osteostimulation using β-CaSiO3/β-Ca3(PO4)2 composite bioceramics, Acta Biomater. 8 (2012) 350–360, https://doi.org/10.1016/j.actbio.2011.08.019.
[32] K. Lin, L. Xia, H. Li, X. Jiang, H. Pan, Y. Xu, et al., Enhanced osteoporotic bone regeneration by strontium-substituted calcium silicate bioactive ceramics, Biomaterials 34 (2013) 10028–10042, https://doi.org/10.1016/j.biomaterials.2013.09.056.
[33] K. Lin, W. Yuan, L. Wang, J. Lu, L. Chen, Z. Wang, et al., Evaluation of host inflammatory responses of beta-tricalcium phosphate bioceramics caused by calcium pyrophosphate impurity using a subcutaneous model, J. Biomed. Mater. Res. B Appl. Biomater. 99 (2011) 350–358, https://doi.org/10.1002/jbm.b.31906.
[34] S. Xu, K. Lin, Z. Wang, J. Chang, L. Wang, J. Lu, et al., Reconstruction of calvarial defect of rabbits using porous calcium silicate bioactive ceramics, Biomaterials 29 (2008) 2588–2596, https://doi.org/10.1016/j.biomaterials.2008.03.013.
[35] R. P, J. N, L. E, M. E, G. H, P. E, et al., Fetal liver endothelium regulates the seeding of tissue-resident macrophages, Nature 538 (2016) 392–396, https://doi.org/10.1038/nature19814.
[36] S. Saravanan, S. Vimalraj, M. Vairamani, N. Selvamurugan, Role of mesoporous Wollastonite (calcium silicate) in mesenchymal stem cell proliferation and osteoblast differentiation: a cellular and molecular study, J. Biomed. Nanotechnol. 11 (2015) 1124–1138, https://doi.org/10.1166/jbn.2015.2057.
[37] Z. P, M. B, X. S, Z. S, T. H, Z. S, et al., Knockdown of Burton's tyrosine kinase confers potent protection against sepsis-induced acute lung injury, Cell Biochem. Biophys. 70 (2014) 1265–1275, https://doi.org/10.1007/s12013-014-0050-1.
[38] Z. P, W. J, X. Y, Y. Y, Z. H, X. S, et al., Loading BMP-2 on nanostructured hydroxyapatite microspheres for rapid bone regeneration, Int. J. Nanomed. 13 (2018) 4083–4092, https://doi.org/10.2147/ijn.S158280.
[39] H. Xt, L. X, X. Y, Y. Y, W. Rx, S. Hh, et al., Building capacity for macrophage modulation and stem cell recruitment in high-stiffness hydrogels for complex periodontal regeneration: experimental studies in vitro and in rats, Acta Biomater. 88 (2019) 162–180, https://doi.org/10.1016/j.actbio.2019.02.004.
[40] E.C. Walker, N.E. Mcgregor, I.J. Poulton, M. Solano, S. Pompolo, T.J. Fernandes, et al., Oncostatin M promotes bone formation independently of resorption when signaling through leukemia inhibitory factor receptor in mice, J. Clin. Invest. 120 (2010) 582–592, https://doi.org/10.1172/Jci40568.
[41] H.L. Herd, K.T. Bartlett, J.A. Gustafson, L.D. Mcgill, H. Ghandehari, Macrophage silica nanoparticle response is phenotypically dependent, Biomaterials 53 (2015) 574–582, https://doi.org/10.1016/j.biomaterials.2015.02.070.
[42] C. Wang, B. Chen, W. Wang, X. Zhang, T. Hu, Y. He, et al., Strontium released bilineage scaffolds with immunomodulatory properties induce a pro-regenerative environment for osteochondral regeneration, Mater. Sci. Eng. C Mater. Biol. Appl. 103 (2019) 109833, https://doi.org/10.1016/j.msec.2019.109833.
[43] M.J. Coathup, S. Samizadeh, Y.S. Fang, T. Buckland, K.A. Hing, G.W. Blunn, The osteoinductivity of silicate-substituted calcium phosphate, J. Bone Joint Surg. Am. 93 (2011) 2219–2226, https://doi.org/10.2106/JBJS.I.01623.
[44] Han Pingping, Wu Chengtie, Xiao Yin, The effect of silicate ions on proliferation, osteogenic differentiation and cell signalling pathways (WNT and SHH) of bone marrow stromal cells, Biomater. Sci. 1 (2013) 379–392, https://doi.org/10.1039/c2bm00108j.
[45] E.J. Kim, S.Y. Bu, M.K. Sung, M.H. Kang, M.K. Choi, Analysis of antioxidant and anti-inflammatory activity of silicon in Murine macrophages, Biol. Trace Elem. Res. 156 (2013) 329–337, https://doi.org/10.1007/s12011-013-9829-y.
[46] K. Li, Y. Xue, T. Yan, L. Zhang, Y. Han, Si substituted hydroxyapatite nanorods on Ti for percutaneous implants, Bioact. Mater. 5 (2020) 116–123, https://doi.org/10.1016/j.bioactmat.2020.01.001.
[47] E.J. Kim, S.Y. Bu, M.K. Sung, M.K. Choi, Effects of silicon on osteoblast activity and bone mineralization of MC3T3-E1 cells, Biol. Trace Elem. Res. 152 (2013) 105–112, https://doi.org/10.1007/s12011-012-9593-4.
[48] I.D. Xynos, A.J. Edgar, L.D. Buttery, L.L. Hench, J.M. Polak, Gene-expression profiling of human osteoblasts following treatment with the ionic products of Bioglass 45S5 dissolution, J. Biomed. Mater. Res. 55 (2015) 151–157, https://doi.org/10.1002/1097-4636(200105)55:2<151::aid-jbm1001>3.0.co;2-d.
[49] T. Gao, H.T. Aro, H. Ylanen, E. Vuorio, Silica-based bioactive glasses modulate expression of bone morphogenetic protein-2 mRNA in Saos-2 osteoblasts in vitro, Biomaterials 22 (2001) 1475–1483, https://doi.org/10.1016/s0142-9612(00)00288-x.
[50] A. Oryan, S. Alidadi, Reconstruction of radial bone defect in rat by calcium silicate biomaterials, Life Sci. 201 (2018) 45–53, https://doi.org/10.1016/j.lfs.2018.03.048.
[51] J. Sun, L. Wei, X. Liu, J. Li, B. Li, G. Wang, et al., Influences of ionic dissolution products of dicalcium silicate coating on osteoblastic proliferation, differentiation and gene expression, Acta Biomater. 5 (2009) 1284–1293, https://doi.org/10.1016/j.actbio.2008.10.011.
[52] W. Liu, T. Wang, C. Yang, B. Darvell, J. Wu, K. Lin, et al., Alkaline biodegradable implants for osteoporotic bone defects–importance of microenvironment pH, Osteoporos. Int. 27 (2016) 93–104, https://doi.org/10.1007/s00198-015-3217-8 a journal established as result of cooperation between the European Foundation for Osteoporosis and the National Osteoporosis Foundation of the USA.
[53] Y. Shen, W. Liu, K. Lin, H. Pan, B. Darvell, S. Peng, et al., Interfacial pH: a critical factor for osteoporotic bone regeneration, Langmuir ACS J. Surf. Colloids 27 (2011) 2701–2708, https://doi.org/10.1021/la104876w.
[54] A. Shioi, M. Katagi, Y. Okuno, K. Mori, S. Jono, H. Koyama, et al., Induction of bone-type Alkaline phosphatase in human vascular smooth muscle cells roles of tumor necrosis factor-α and oncostatin M derived from macrophages, Circ. Res. 91 (2002) 9–16, https://doi.org/10.1161/01.res.0000026421.61398.f2.
[55] D.H. Kim, K.C. Lee, S.Y. Han, Cyclosporin A aggravates calcification of vascular smooth muscle cells under high-glucose conditions with a calcifying medium, Ann. Transplant. 23 (2018) 112–118, https://doi.org/10.12659/aot.908168.
[56] T.J. Fernandes, J.M. Hodge, P.P. Singh, D.G. Eeles, F.M. Collier, H. Ian, et al., Cord blood-derived macrophage-lineage cells rapidly stimulate osteoblastic maturation in mesenchymal stem cells in a glycoprotein-130 dependent manner, PLoS One 8 (2013), https://doi.org/10.1371/journal.pone.0073266 e73266.

[57] X.T. He, R.X. Wu, X.Y. Xu, J. Wang, Y. Yin, F.M. Chen, Macrophage involvement affects matrix stiffness-related influences on cell osteogenesis under three-dimensional culture conditions, Acta Biomater. 71 (2018) 132–147, https://doi.org/10.1016/j.actbio.2018.02.015.

[58] K.L. Spiller, R.R. Anfang, K.J. Spiller, J. Ng, K.R. Nakazawa, J.W. Daulton, et al., The role of macrophage phenotype in vascularization of tissue engineering scaffolds, Biomaterials 35 (2014) 4477–4488, https://doi.org/10.1016/j.biomaterials.2014.02.012.

[59] G. P, D. Y, B. B, D. E, B. R, D. J, et al., Induction of osteogenesis in mesenchymal stem cells by activated monocytes/macrophages depends on oncostatin M signaling, Stem cells (Dayton, Ohio) 30 (2012) 762–772, https://doi.org/10.1002/stem.1040.

[60] T. Mg, C. Yw, S. My, Macrophage-mediated osteogenesis activation in co-culture with osteoblast on calcium silicate cement, J. Mater. Sci. Mater. Med. 26 (2015) 276, https://doi.org/10.1007/s10856-015-5607-z.

[61] S.A. Villalta, H.X. Nguyen, B. Deng, T. Gotoh, J.G. Tidball, Shifts in macrophage phenotypes and macrophage competition for arginine metabolism affect the severity of muscle pathology in muscular dystrophy, Hum. Mol. Genet. 18 (2009) 482–496, https://doi.org/10.1093/hmg/ddn376.

[62] S. Gea-Sorli, R. Guillamat, A. Serrano-Mollar, D. Closa, Activation of lung macrophage subpopulations in experimental acute pancreatitis, J. Pathol. 223 (2011) 417–424, https://doi.org/10.1002/path.2814.

[63] J. Capote, I. Kramerova, L. Martinez, S. Vetrone, E.R. Barton, H.L. Sweeney, et al., Osteopontin ablation ameliorates muscular dystrophy by shifting macrophages to a pro-regenerative phenotype, J. Cell Biol. 213 (2016) 2135OIA35, https://doi.org/10.1083/jcb.201510086.

[64] N. Jetten, M.M. Donners, A. Wagenaar, J.P. Cleutjens, N. van Rooijen, M.P. de Winther, et al., Local delivery of polarized macrophages improves reperfusion recovery in a mouse hind limb ischemia model, PLoS One 8 (2013), https://doi.org/10.1371/journal.pone.0068811 e68811.

[65] X. S, L. K, W. Z, C. J, W. L, L. J, et al., Reconstruction of calvarial defect of rabbits using porous calcium silicate bioactive ceramics, Biomaterials 29 (2008) 2588–2596, https://doi.org/10.1016/j.biomaterials.2008.03.013.